Nonlinear Thermoelectricity in Disordered Nanowires

K. A. Muttalib and Selman Hershfield

Department of Physics, University of Florida, Gainesville, Florida 32611-8440, USA

(Received 6 February 2015; revised manuscript received 27 March 2015; published 8 May 2015)

The creation of efficient thermoelectric devices remains a technological challenge. Using nanoscale-engineered devices offers some potential advantages over bulk materials; however, they also present new problems. The microscopic Hamiltonian of a device which optimizes the efficiency and power output for a particular load and temperature profile is not necessarily optimum for another temperature difference and external load. Furthermore, one cannot necessarily manufacture a particular Hamiltonian. In this paper, we calculate the nonlinear thermoelectric transport through a gate-modulated one-dimensional disordered semiconducting nanowire connected to two large leads. The disorder is chosen to be Lorentzian, which allows exact results for transmission through the wire for all strengths of disorder. By tuning the gate voltage acting on the nanowire, we show that the thermodynamic efficiency can be made large enough to be industrially competitive. The gate voltage allows one to maximize the efficiency and power output for particular temperature differences between the leads as well as different external loads.

DOI: 10.1103/PhysRevApplied.3.054003

I. INTRODUCTION

Thermoelectricity, converting unused waste heat to electricity or using electricity for refrigeration, has gained increased attention in recent years. For example, as much as 75% of the energy generated by a car's internal-combustion engine ends up lost as waste heat [1]. Because bulk materials turn out to be inherently inefficient [2,3], the actual number of commercial applications of thermoelectricity has remained limited. Recent progress in nano-engineered materials has opened the possibility to build thermoelectric materials with specific properties to boost the efficiency [4–12].

One class of nanostructured devices with yet-unrealized potential for higher efficiency consists of two large leads at different temperatures connected by a molecule [13–19], wire [20–23], or quantum dot [24–28]. The electrical current and heat flow for these systems is determined by the transmission across the connecting region. From earlier work on these systems [29] we know that for tunneling through a single-resonant level the efficiency can approach the maximum thermodynamic efficiency (Carnot limit), but only in the limit where the power output also goes to zero. In the nonlinear-response regime, which is easy to obtain in these small systems, one can have finite power output at very high efficiency [29–35]. By placing many of these nanodevices in parallel one can scale up the power to macroscopic levels.

While this is quite promising, there are serious problems from an application point of view. First, while the Hamiltonians for the central systems may be physically reasonable for tunneling through certain kinds of molecules, there is no guarantee that a particular optimum-transmission coefficient will actually be realizable in a molecular system. Second, and perhaps more important, the optimum transmission as a function of energy depends on both the temperature difference between the two sides of the system and also the external load for the thermoelectric generator. Thus, if one is lucky enough to find just the right molecule for tunneling through for a particular temperature gradient and external load, the same device may not be optimum for a different temperature difference or external load.

Both of these issues, reliable manufacturing and optimization under varying conditions, may be solvable with semiconducting nanowires. Semiconducting nanowires can be manufactured reproducibly. By applying a gate to the wires one can also tune the transmission probability as a function of energy, allowing for different operating conditions. Indeed, in a recent preprint Brovman *et al.* [36] have measured a large Seebeck coefficient in silicon nanowires. The Seebeck coefficient measures the thermoelectric voltage in response to a temperature gradient. It is one of the parameters that enters into the linear-response figure of merit for thermoelectric generators. According to the Mott formula [37] the Seebeck coefficient is maximized for a rapidly varying conductance or transmission coefficient near the Fermi energy. Brovman *et al.* achieved their large Seebeck coefficient by using the gate voltage to place the Fermi energy near the impurity band of the nanowire.

In the nonlinear-response regime, the criterion for maximizing efficiency is more complicated. It is not sufficient to just have a rapidly varying transmission probability or density of states near the equilibrium Fermi energy. As will be discussed in the next section, there is an energy $\hat{E}$ that depends on the temperature differences and the operating voltage. To maximize the efficiency and power output, one would like the

transmission to be large above $\hat{E}$ and small below it. Such a transmission as a function of energy can be achieved for some models of molecular tunnel junctions [29,38]; however, this relies on subtle interference effects that require careful tuning of the parameters of the Hamiltonian for particular operating conditions.

In this paper we show that the efficiency and power output can be optimized more robustly for semiconducting nanowire with an external gate. We consider a model of a gate-modulated semiconductor nanowire device and show that the ideas of Ref. [29] about the interplay of the microscopic and thermodynamic parameters can be implemented by using the gate voltage V_g as a tuning parameter. We calculate the full nonlinear thermodynamic efficiency η and power output P as a function of the gate-voltage parameter $U_g = -eV_g$. We will show explicitly that for a given set of microscopic parameters of the disordered wire and thermodynamic parameters of the leads, the relative efficiency η/η_c, where η_c is the Carnot efficiency, can be increased from zero to $\eta/\eta_c > 0.5$ by simply changing the gate voltage. The results should be insensitive to incoherent processes, and should remain valid for large temperature and voltage gradients relevant for practical devices.

The rest of the paper is organized as follows. In Sec. II we briefly review the idea of the interplay of thermodynamic and microscopic parameters as proposed in Ref. [29]. In Sec. III we describe the complete model system, consisting of one-dimensional (1D) disordered nanowire plus three-dimensional (3D) leads. We first explain how the gate modulation allows for a simple and effective implementation of the interplay described in Sec. II. We then obtain an exact expression for the transmission function across the wire in terms of the impurity-averaged Green's function of a 1D disordered wire and the surface Green's function of a 3D perfectly conducting lead. In Sec. IV this transmission function is used to evaluate the efficiency and power output of the model device as a function of the external gate voltage. In Sec. V we summarize the results and briefly discuss the issues not covered in this work.

II. INTERPLAY OF THERMODYNAMIC AND MICROSCOPIC PARAMETERS

In the linear-response regime, a large efficiency of the thermoelectric device at temperature T is obtained when the figure of merit ZT defined as

$$ZT \equiv \frac{TGS_e^2}{\kappa} \tag{2.1}$$

is large, where G and κ are the electrical and thermal conductances, respectively. The thermopower or Seebeck coefficient S_e can be written in the low-temperature limit, in the absence of interactions, as

$$S_e = \frac{\pi^2}{3}\frac{k_B}{e}(k_BT)\frac{d}{dE}\ln \mathcal{T}(E)|_{E=E_F}, \tag{2.2}$$

where $\mathcal{T}(E)$ is the energy-dependent transmission function. Thus, in the linear-response regime a large ZT or a large S_e require a large variation of $\mathcal{T}(E)$ at the Fermi energy. This was used in Ref. [36] to argue that the large S_e in the experiment resulted from a large variation of the conductance near the band edge.

In contrast, as shown in Ref. [29], this is not a necessary or sufficient condition in the *nonlinear regime*, which is more appropriate for nanodevices with large temperature and voltage gradients. In the absence of interactions, the power output should be written in terms of $\mathcal{T}(E)$ as

$$P = (\mu_R - \mu_L)I_N; \qquad I_N \equiv \frac{1}{h}\int dE\mathcal{T}(E)F(E);$$
$$F(E) \equiv f_L(\mu_L, T_L; E) - f_R(\mu_R, T_R; E). \tag{2.3}$$

Here, I_N is the number current and $f_j(\mu_j, T_j; E) \equiv 1/(1 + e^{(E-\mu_j)/k_BT_j})$, $j = (L, R)$, are the Fermi functions in the left (hot) and right (cold) leads. Note that while the so-called thermopower or Seebeck coefficient S_e is an intensive quantity, the actual power P defined in (2.3) is an extensive quantity and therefore can be scaled up. Using $\mathcal{T}(E)$ the efficiency can be written as ($T_L > T_R$)

$$\eta = \frac{(\mu_R - \mu_L)\int dE\mathcal{T}(E)F(E)}{\int dE(E-\mu_L)\mathcal{T}(E)F(E)}. \tag{2.4}$$

This expression, together with Eq. (2.3), allows us to optimize the efficiency as well as the power output by carefully matching $\mathcal{T}(E)$ for a given $F(E)$. Since $F(E)$ changes sign at $\hat{E}$ given by $F(\hat{E}) = 0$, or

$$\hat{E} = \frac{T_L\mu_R - T_R\mu_L}{T_L - T_R}, \tag{2.5}$$

the ideal $\mathcal{T}(E)$ turns out to be a square wave [29,30]. While the lower edge of the square wave that maximizes the efficiency for a given fixed power has been calculated in Ref. [30], it is more useful for our purposes to obtain large power and high efficiency simultaneously, to maximize the number current I_N by choosing the lower edge at $\hat{E}$. In this case the negative value of $F(E)$ for $E < \hat{E}$, which reduces the contribution to the number current in the positive direction, is minimized by allowing transmission only for $E > \hat{E}$. In practice, this requires a mechanism to reduce $\mathcal{T}(E)$ for $E < \hat{E}$ as much as possible. The t-stub model considered in Ref. [29] relies on the destructive interference from two possible paths to provide this reduction. We will show below that a nanowire-lead system with a tunable gate voltage can provide a simple, efficient, and practically robust way of obtaining the same goal.

III. THE NANOWIRE-LEAD SYSTEM

A semiconductor nanowire system similar to that used in Ref. [36] has the possibility to provide the crucial feature that $\mathcal{T}(E)$ is negligible for $E < \hat{E}$, without depending on subtle quantum effects such as interference. This is possible by taking advantage of the band structure of the wire-lead system and the fact that the impurity band of the wire can be adjusted by the applied gate voltage. Figure 1 shows the sketch of our proposed device with external gate voltage, consisting of many parallel wires. Each can be considered as quasi-1D wires, and not coupled to each other. We can therefore calculate the transmission function and the resulting thermoelectric efficiency and power output for one wire, and as shown in Ref. [29], essentially scale up the power output by multiplying by the number of wires without compromising the efficiency.

For explicit calculations, we will choose each of our nanowires to be effectively 1D with hopping parameter t_w and strength of disorder W. We note that for a strictly 1D (single "channel") disordered wire, the localization length is equal to the mean free path. A thin but multichannel wire remains "quasi 1D" as long as the width remains much smaller than the localization length, which is given by the mean free path multiplied by the number of transverse transmission channels. Without inelastic scattering a wire with N channels can be mapped onto N-independent 1D models with renormalized parameters. For small N we expect the transmission functions for the modes to be similar. In such an effectively 1D model the impurity band will be restricted to $E_L^0 \le E \le E_U^0$, where $E_L^0 = (-2t_w - W/2)$ and $E_U^0 = (2t_w + W/2)$ are the lower and upper impurity-band edges, respectively, in the absence of an external gate voltage. The source and the drain can be considered as 3D perfectly conducting semi-infinite leads on the left (L) and right (R) that act as reservoirs at temperatures T_L and T_R, respectively. The 3D conduction band of the leads is within the range $[-6t, 6t]$, where $t = t_L = t_R$ is the tight-binding hopping parameter in each of the leads, assumed to be symmetric for simplicity. When a gate voltage V_g is applied on the wire, the impurity band is shifted relative to the conduction band by $U_g = -eV_g$.

As shown in Fig. 2, the edges of the impurity band now depend on the gate voltage, and the transmission from the left lead will be blocked for all $E < E_L$ or $E > E_U$, where $E_L = (E_L^0 + U_g)$ and $E_U = (E_U^0 + U_g)$ are the lower and upper impurity-band edges, respectively, in the presence of the external gate voltage. In other words, the gate voltage can be used to tune the position of the lower band edge (determined by the microscopic parameters of the wire), with respect to the value of $\hat{E}$ (determined by the parameters of the reservoirs).

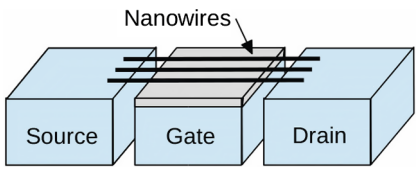

FIG. 1. Sketch of the device, consisting of many parallel nanowires with an external gate voltage.

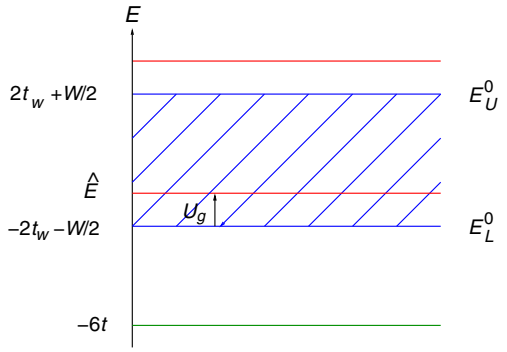

FIG. 2. Sketch of the band structure for a 1D wire connected to 3D leads. The 3D conduction band of the leads allows the range $-6t < E < 6t$. The 1D impurity band of the nanowire (shaded blue), on the other hand, is restricted from $E_L^0 = (-2t_w - W/2) \le E \le E_U^0 = (2t_w + W/2)$ in the absence of the applied gate voltage. The thermodynamic parameters fix $\hat{E}$, which we take to lie somewhere within the impurity band. The applied voltage V_g can then be tuned to shift the lower impurity-band edge by $U_g = -eV_g$ such that $(E_L^0 + U_g) = \hat{E}$.

In particular, let us suppose the 1D wire consists of N sites with lattice spacing a, connected to the leads by symmetric couplings $V_L = V_R = V$, where V_L connects site 1 with the left lead and V_R connects site N with the right lead. Then the (retarded) Green's function G of the wire connected to the semi-infinite leads is given [39] in terms of the (retarded) Green's function G^0 of the isolated wire by a 2×2 matrix

$$G^{-1} = (G^0)^{-1} - \Sigma^0 I_2; \qquad \Sigma^0 = |V|^2 g^0, \tag{3.1}$$

where I_2 is a 2×2 identity matrix and $g^0 = g_L^0 = g_R^0$ is the surface Green's function of the isolated semi-infinite lead. The relevant off-diagonal element of the full connected Green's function is then given by

$$G_{1N} = \frac{G_{1N}^0}{(\alpha_0 + \beta_0)(\alpha_0 - \beta_0)}, \tag{3.2}$$

where $\alpha_0 \equiv 1 - G_{NN}^0 \Sigma^0$ and $\beta_0 \equiv G_{1N}^0 \Sigma^0$. Here G_{11}^0 and G_{NN}^0 are the diagonal elements of G^0, the 2×2 Green's function of the isolated wire of length $L = Na$, and G_{1N}^0 and G_{N1}^0 are the corresponding off-diagonal elements.

The transmission function can then be obtained from

$$\mathcal{T}(E) = \mathrm{Tr}[\Lambda_L G_{1N} \Lambda_R G_{1N}^\dagger], \tag{3.3}$$

and the incoming and outgoing velocities are included in the functions

$$\Lambda_L = \Lambda_R \equiv \Lambda = -2\mathrm{Im}[\Sigma^0] = -2|V|^2\mathrm{Im}[g^0]. \quad (3.4)$$

Thus, the main task in calculating the power output or the thermoelectric efficiency as given in Eqs. (2.3) and (2.4) reduces to evaluating the Green's functions G^0_{1N} and G^0_{NN} for an isolated 1D disordered wire and the surface Green's function g^0 of the isolated semi-infinite 3D leads. The interplay with thermodynamic parameters will be possible once a gate voltage is applied to the wire.

A. Model for the one-dimensional disordered wire

For a 1D disordered wire, the Lloyd model [40] with a Lorentzian distribution of disorder is exactly solvable for the transmission function $\mathcal{T}(E)$ needed for the thermoelectric properties. We therefore choose a Lorentzian distribution for our disordered nanowire and use the known Green's functions for the Lloyd model to evaluate the transmission as a function of energy. We choose the Hamiltonian of the nanowire with N sites to be the standard tight-binding model:

$$H = -t_w \sum_{i=1}^{N-1}(c_i^\dagger c_{i+1} + \mathrm{H.c.}) + \sum_{i=1}^{N} \epsilon_i c_i^\dagger c_i, \quad (3.5)$$

where $c_i^\dagger$ and c_i are the creation and annihilation operators of an electron at site i in the nanowire and t_w is the hopping energy. The site energy ϵ_i is random, assumed to have a distribution of the form

$$P(\epsilon_i) = \frac{1}{\pi}\frac{W}{\epsilon_i^2 + W^2}, \quad (3.6)$$

where W is the width of the distribution. We will assume that the energy band of the wire is broadened from $-2t_w < E < 2t_w$ to $(-2t_w - W/2) < E < (2t_w + W/2)$ as in the case of box disorder with width W. The disorder-averaged Green's function is given by [41]

$$\langle G(z)\rangle = (zI_N - F)^{-1}, \quad (3.7)$$

where I_N is the $N \times N$ identity matrix and

$$F_{m,n} = -iW\delta_{m,n} + t_w(\delta_{m,n+1} + \delta_{m,n-1}). \quad (3.8)$$

The matrix $(zI_N - F)$ is tridiagonal and symmetric, and can be inverted analytically [42]. The results are

$$G^0_{11} = G^0_{NN} = -\frac{1}{t_w}\frac{\sin N\theta}{\sin(N+1)\theta};$$
$$G^0_{1N} = (-1)^{N+1}\frac{1}{t_w}\frac{\sin\theta}{\sin(N+1)\theta}, \quad (3.9)$$

where $\cos\theta = (z + iW)/(-2t_w)$ and we add a superscript zero to indicate that this is the Green's function when the wire is still isolated, not connected to any leads. Separating the real and imaginary parts $\theta = \phi + i\gamma$ and replacing $z = E$, we get

$$\cos\phi(E) = -2E/\Gamma(E); \qquad \cosh\gamma(E) = \Gamma(E)/(4t_w);$$
$$\Gamma(E) \equiv \sqrt{E_+^2 + W^2} + \sqrt{E_-^2 + W^2}, \quad (3.10)$$

where $E_\pm \equiv 2t_w \pm E$. In the large N limit, the Green's functions can be simplified. In this limit we can identify the parameter γ with the inverse localization length, from the N dependence of $|G^0_{1N}|^2$, given by

$$|G^0_{1N}|^2 \to \frac{4}{t_w^2}[\cosh^2\gamma - \cos^2\phi]e^{-2(N+1)\gamma}. \quad (3.11)$$

This result implies an exponential decay of the transmission probability, in the form $\exp[-L/\xi]$, where $L = Na$ is the length of the wire and ξ is the localization length, a being the lattice spacing. Thus, we identify

$$\frac{a}{\xi(E)} \equiv \gamma(E). \quad (3.12)$$

We note that the localization length at $E = 0$ is given by

$$\xi_0 \equiv \frac{a}{\gamma(E=0)} = \frac{1}{\cosh^{-1}[\sqrt{1 + (W/2t_w)^2}]}. \quad (3.13)$$

B. Perfectly conducting 3D leads

The surface Green's function of the 3D leads is given by

$$g^0(E) = \int_0^\pi \frac{dk_x}{\pi}\int_0^\pi \frac{dk_y}{\pi} g^0_{1D}(E + 2t\cos k_x + 2t\cos k_y), \quad (3.14)$$

where t is the hopping parameter in the leads. Here g^0_{1D} is the surface Green's function of a one-dimensional lead given by

$$g^0_{1D}(|E| \le 2t) = -\frac{1}{t}\left(\frac{E}{-2t} + iE_t\right);$$
$$g^0_{1D}(|E| \ge 2t) = -\frac{1}{t}\left(\frac{E}{-2t} + \mathrm{sgn}(E)E_t\right), \quad (3.15)$$

where $E_t \equiv \sqrt{1 - (E/2t)^2}$. It is possible to use the full integral for $g^0(E)$ to evaluate the transmission function, but it turns out that a very simple analytic expression approximates the integral in the range away from the 3D band edge, where the transmission function is non-negligible. In particular, for $|E| \le 3t$ one can use, to a very good approximation, $\mathrm{Re}[g^0] \approx \sin(E/2)/3t$ and

$\mathrm{Im}[g^0] \approx (\pi/6b)(b - E^2)$, where $b \equiv (9\pi^2)/(\pi^2 - 3\sqrt{3})$. While the imaginary part has a $|E/t|^{3/2}$ dependence and the real part falls off as $1/|E|$ near the band edges at $E \approx \pm 6t$, we will see that for our choice of the parameters the impurity band restricts the transmission within an even smaller range. This will allow us to use the above simple forms in our evaluations of the efficiency and power output.

C. Transmission function

For large N, G^0_{1N} is exponentially small compared to G^0_{NN}, so that in the expression for G_{1N} in Eq. (3.2), we can neglect G^0_{1N} compared to G^0_{NN}. Then $G_{1N} \approx G^0_{1N}/\alpha_0^2$. The final expression for transmission function then becomes

$$\mathcal{T}(E) \approx \frac{4|V|^4}{d^2}(\mathrm{Im}[g^0])^2 |G^0_{1N}|^2, \tag{3.16}$$

where

$$d \equiv 1 + \lambda^2 |g^0|^2 + 2\lambda(\mathrm{Re}[g^0]\cos\phi - \mathrm{Im}[g^0]\sin\phi);$$
$$\lambda \equiv \frac{|V|^2}{t_w} e^{-\gamma}. \tag{3.17}$$

IV. EFFICIENCY AND POWER OUTPUT: TUNING BY GATE VOLTAGE

When a gate voltage V_g is applied to the wire, all E in the wire are shifted by the energy $U_g = -eV_g$ but the lead energies are not. Thus, we need to replace E by $E + U_g$ in the expression for G^0_{1N} of the isolated wire, but energy in g^0 of the isolated leads remains unshifted. In order to understand how this affects the interplay of the microscopic and the thermodynamic parameters, we will choose an explicit example. All energies will be denoted in units of t. We will consider the relative efficiency η/η_c, where $\eta_c \equiv 1 - T_R/T_L$ is the Carnot efficiency. The power P will be described in units of t^2/h.

As an explicit example, let us choose a nanowire of length $L = N = 20$ (lattice spacing $a = 1$) with hopping parameter $t_w = 1$ and Lorentzian disorder characterized by $W = 0.01$. This corresponds to the localization length $\xi_0 \sim 10L$ so that it can be considered as weak disorder. The wire is connected to the leads by a coupling $V = 0.5$. Our choice of the microscopic parameters of the wire then fixes the lower impurity-band edge at $E^0_L = (-2t_w - W/2) = -2.005$.

We now need the thermodynamic parameters. Ideally, one would like to have the cold (right) lead to be at room temperature ($T_R \sim 300$ K) and the hot (left) lead to be at $T_L \sim 450$ K, such that the Carnot efficiency $\eta_c \equiv 1 - T_R/T_L \sim 1/3$. We take $T_L = 0.3t$ and $T_R = 0.2t$, which gives the same Carnot efficiency. For simplicity, we will choose $\mu_L = -1.75$ and $\mu_R = -1.5$, although in practice one of them will be fixed by the load connected to the thermoelectric device. This fixes the characteristic energy $\hat{E} = -1.0$, which is above the lower impurity-band edge, as shown in Fig. 2.

Applying a gate voltage V_g shifts all of the energies in the impurity band of the wire by U_g relative to the conduction band of the lead. Figure 3 shows the power output and the efficiency of the nanowire system, for the above-chosen set of parameters, as a function of U_g. Several features are important. First, the relative efficiency η/η_c can be tuned by the gate voltage from zero to almost 0.6, keeping in mind that $\eta/\eta_c > 0.3$ is expected to be industrially competitive [29]. Second, the maximum of the relative efficiency occurs at $U_g = 1.005$, where the lower impurity-band edge is pushed up from $(-2t_w - W/2) = -2.005$ to $(-2t_w - W/2 + Ug) = -1$, which coincides with $\hat{E}$. As shown in Fig. 4, for this choice of U_g all negative contributions to the number current [see Eq. (2.3)] due to the negative values of $F(E)$ are now cut off by the band edge. Finally, the power output is also a maximum near the same value of U_g, so both efficiency and power can be optimized simultaneously. There is a broad range of values of the gate voltage corresponding to $0.85 \le U_g \le 1.2$ (in units of t) for which the efficiency is larger than $0.5\eta_c$ and the power is larger than 5×10^{-4} (in units of t^2/h).

As noted above, both power output and the efficiency peak around the same value of $U_g \approx 1$. However, the absolute value of the power output P for a single wire is clearly very small and practical applications will require many orders of magnitude larger values for P. For the present model, this means that in Fig. 1, the number of wires should be sufficiently large. At the same time, the

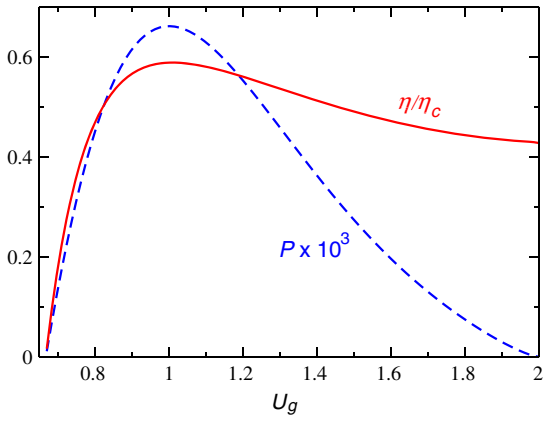

FIG. 3. Relative efficiency η/η_c (red solid curve) and power output P (blue dashed curve) as a function of gate-voltage parameter $U_g = -eV_g$ for the set of microscopic and thermodynamic parameters as chosen in the text. The disorder is chosen to be weak, given by $L \sim 0.1\xi_0$. The maximum efficiency occurs at $U_g = 1.005$, for which the lower impurity-band edge coincides with $\hat{E}$. For $0.85 \le U_g \le 1.2$ the device can be considered optimal.

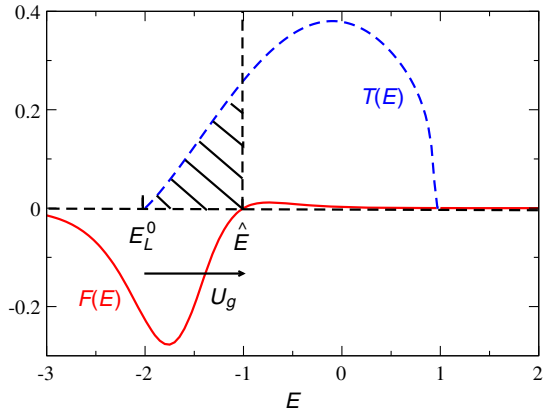

FIG. 4. Transmission function $\mathcal{T}(E)$ (blue dashed curve) and difference of Fermi functions $F(E)$ (red solid curve) for the same set of parameters as chosen in Fig. 3, the gate-voltage parameter being fixed at $U_g = 1.005$ where the efficiency is maximum. The lower impurity-band edge at $E_L^0 = -2.005$ in the absence of V_g is shifted to $\hat{E}$ for $U_g = 1.005$, such that all negative contributions to the number current arising from negative values of $F(E)$ are now cut off by the band edge.

distances between the wires also need to be sufficiently large in order to keep them from interacting with one another. We estimate that putting parallel wires 10 nm apart in a 3D array will result in $P \sim 6\times10^{-4}\times(t^2/h)/(10^{-8}\,\mathrm{m})^2 \sim 4\times10^6\,\mathrm{W/m^2}$. Here, supplying all proper units, we use $k_B T_R = 0.2t$, where k_B is the Boltzmann constant and $T_R = 300$ K. This is orders of magnitude larger than currently available commercial devices, although it requires a gate voltage applied to multiple layers as opposed to a single layer of wires shown in Fig. 1. Of course, P would be smaller if, e.g., the wire-lead coupling V is weaker, or if the

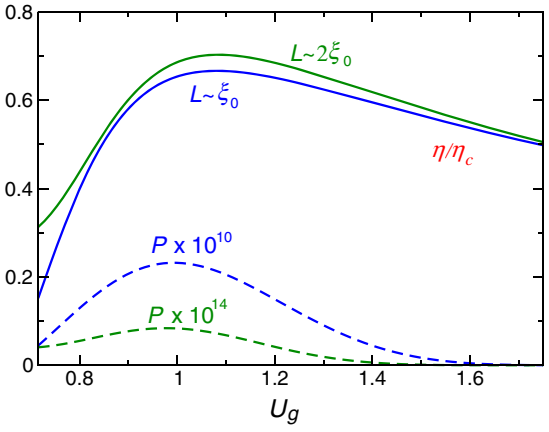

FIG. 5. Relative efficiency η/η_c (solid blue and green lines) and power output P (dashed blue and green lines) as a function of gate-voltage parameter U_g for the same set of microscopic and thermodynamic parameters as chosen in Fig. 3, but for different lengths of the wire. The blue lines correspond to $L \sim \xi_0$ while the green lines correspond to $L \sim 2\xi_0$.

disorder of the wire is stronger, than the values chosen here. In Fig. 5, we show efficiency and power for two much longer wires, with $L \sim \xi_0$ and $L \sim 2\xi_0$, compared to the chosen value $L \sim \xi_0/10$ in Fig. 3. Here ξ_0 is the localization length. Note that L/ξ_0 is a measure of disorder, such that for a fixed width of the distribution W, longer wires imply stronger disorder ($L/\xi_0 > 1$ correspond to the localized regime). Since the transmission function decreases with increasing disorder, the power output decreases significantly, as shown in Fig. 5. However, the efficiency remains high because apparently in the ratio, the number and heat currents largely cancel out the disorder effects. (It is not clear why the peak efficiency slightly *increases* with increasing disorder.) Thus, weaker disorder is needed not for higher efficiency, but for larger power output. We mention that the total power also depends on how close the wires can be put together. On the other hand, the results are largely insensitive to incoherent scatterings or nonuniformity of the wires.

V. SUMMARY AND OUTLOOK

In this paper we present calculations to demonstrate that gated semiconducting nanowires are excellent candidates for high efficiency and power thermoelectric devices. Our model consists of an effectively one-dimensional disordered semiconducting nanowire connected to three-dimensional leads. We emphasize that the theoretical model considered here is not just a toy model, but is relevant for actual devices. For example, for our purposes a disordered wire is effectively one dimensional as long as the localization length ξ_0 is much larger than the width of the wire. For a wire with length $L = 1$ μm and $L/\xi_0 = 10$, this means that wires with width $\sim$10 nm are effectively 1D. Such wires can be easily made with current technology [21]. The disorder in the wire is assumed to be Lorentzian, which allows us to calculate the transmission function $\mathcal{T}(E)$ through the wire exactly. However, we expect that more realistic types of disorder will only change some numbers like the power output by a small factor, but the important result that the efficiency is largely independent of disorder, as shown in Fig. 5, will remain valid. The maximum efficiency and power output occur when the transmission function is large for energies greater than $\hat{E}$ and small for energies less than $\hat{E}$. The energy scale $\hat{E}$ depends on the temperature difference between the leads and the operating voltage. Through the application of a gate voltage the transmission function $\mathcal{T}(E)$ may be adjusted to have this property. As Fig. 3 shows, there is a wide range of values for the gate voltage where a single-wire device can be "optimal," with efficiency $\eta/\eta_c > 0.5$ and the power output $P > 5\times10^{-4}(t^2/h)$ per wire. It should then be possible to increase the power by connecting many wires in parallel, without compromising the efficiency. The operation should be robust against incoherent processes, and

should remain valid at arbitrary temperature or voltage gradients. We note that the ideas presented here can also be implemented using parallel 2D sheets instead of a 3D array of nanowires.

One factor that we have not included in the current work is the magnitude of the phonon thermal conductance. We assume that the heat current is carried entirely by the electrons. In general, the phonon contribution to the thermal conductance $\kappa_{\rm ph}$ adds to the energy current, reducing the efficiency. However, the present model has two intrinsic advantages. First, it is well known that the surface scattering in a disordered Si nanowire can greatly reduce $\kappa_{\rm ph}$ [22]. Second, in the present geometry, phonon transmission is also greatly reduced due to large reflection from the contact, i.e., a large Kapitza resistance [43,44]. In particular, phonons in the leads with transverse wavelength larger than the cross-sectional dimension of the wire will be backscattered with high probability, reducing the transmission and therefore the thermal conductivity [45,46]. Indeed, Boukai *et al.* [21] measured $\kappa_{\rm ph} = 0.76\ {\rm W}/({\rm m\,K})$ in Si nanowires that are several microns long (L) and 10 nm wide, around temperature $T = 200$ K. This corresponds to $K_{\rm ph} \equiv \kappa_{\rm ph} LT = 7.6 \times 10^{-4}$ W, where for the purpose of definiteness, we chose $L = 5\ \mu$m. These wires are highly doped and as a result "metalliclike" (increasing conductivity with decreasing temperature), so we compare the above value of $K_{\rm ph}$ with the corresponding $K_{\rm el}$ for a weakly disordered wire. For that, we rewrite Eq. (2.4) as $\eta = P/K$, and using the peak values of P and η from Fig. 3 for a weakly disordered wire, we obtain $K = K_{\rm el} \sim 3 \times 10^{-3}$ W (using $\eta_c = 1/3$). Thus, $K_{\rm ph} < K_{\rm el}$, and including the phonon contribution such that $K = K_{\rm el} + K_{\rm ph}$, we find that $\eta/\eta_c \sim 0.48$, which is still larger than 0.3. Thus the phonon thermal conductance can indeed be made small in nanowires. Note that if necessary, disorder can be made weaker by choosing a shorter wire, which also helps limiting any inelastic scattering that might affect the performance of the device. In fact, shorter wires might also be required to operate in the nonlinear regime depending on the load and the leads. Finally, we remark that electron-phonon interactions as well as charging and screening effects can be amplified in the nonlinear regime. Further studies are needed to address these issues.

ACKNOWLEDGMENTS

We thank J.-L. Pichard for stimulating discussions during early stages of this work.

Note added in proof.—A related complementary work appears in this issue (see Ref. [47]) where a similar thermoelectric device consisting of gate-modulated nanowires is considered. It focuses on the strongly disordered phonon-assisted variable range-hopping regime within linear response, as opposed to the weakly disordered wire considered here focusing on the nonlinear regime.

[1] G. P. Meisner, Low cost advanced thermoelectric (TE) technology for automotive waste heat recovery, Bull. Am. Phys. Soc. **59**, 1092 (2014); M. Lucibella, Automotive thermoelectrics, APS News **23**, 1 (2014).
[2] See, e.g., Y. Dubi and M. Di Ventra, Heat flow and thermoelectricity in atomic and molecular junctions, Rev. Mod. Phys. **83**, 131 (2011), and references therein.
[3] G. J. Snyder and E. S. Toberer, Complex thermoelectric materials, Nat. Mater. **7**, 105 (2008).
[4] L. D. Hicks and M. S. Dresselhaus, Effect of quantum well structures on the thermoelectric figure of merit, Phys. Rev. B **47**, 12727 (1993).
[5] L. D. Hicks, T. C. Harman, X. Sun, and M. S. Dresselhaus, Experimental study of the effect of quantum well structure on the thermoelectric figure of merit, Phys. Rev. B **53**, R10493 (1996).
[6] A. Majumdar, Thermoelectricity in semiconductor nanostructures, Science **303**, 777 (2004).
[7] M. Paulsson and S. Datta, Thermoelectric effect in molecular electronics, Phys. Rev. B **67**, 241403(R) (2003).
[8] M. Dresselhaus, G. Chen, M. Y. Tang, R. Yang, H. Lee, D. Wang, Z. Ren, J-P. Fleurial, and P. Gogna, New directions for low-dimensional thermoelectric materials, Adv. Mater. **19**, 1043 (2007).
[9] P. Reddy, S. Y. Jang, R. A. Segalman, and A. Majumdar, Thermoelectricity in molecular junctions, Science **315**, 1568 (2007).
[10] A. Abbout, H. Ouerdane, and C. Goupil, Mesoscopic thermoelectric transport near zero transmission energies, Phys. Rev. B **87**, 155410 (2013).
[11] A. Glatz and I. S. Beloborodov, Thermoelectric performance of granular semiconductors, Phys. Rev. B **80**, 245440 (2009); Thermoelectric performance of weakly coupled granular materials, Europhys. Lett. **87**, 57009 (2009).
[12] K. Wu, L. Rademaker, and J. Zaanen, Bilayer Excitons in Two-Dimensional Nanostructures for Greatly Enhanced Thermoelectric Efficiency, Phys. Rev. Applied **2**, 054013 (2014).
[13] M. Leijnse, M. R. Wegewijs, and K. Flensberg, Nonlinear thermoelectric properties of molecular junctions with vibrational coupling, Phys. Rev. B **82**, 045412 (2010).
[14] P. Murphy, S. Mukerjee, and J. Moore, Optimal thermoelectric figure of merit of a molecular junction, Phys. Rev. B **78**, 161406(R) (2008).
[15] J. Koch, F. von Oppen, Y. Oreg, and E. Sela, Thermopower of single-molecule devices, Phys. Rev. B **70**, 195107 (2004).
[16] O. Karlström, H. Linke, G. Karlström, and A. Wacker, Increasing thermoelectric performance using coherent transport, Phys. Rev. B **84**, 113415 (2011).

[17] J. P. Bergfield, M. A. Solis, and C. A. Stafford, Giant thermoelectric effect from transmission supernodes, ACS Nano **4**, 5314 (2010).
[18] O. Entin-Wohlman, Y. Imry, and A. Aharony, Three-terminal thermoelectric transport through a molecular junction, Phys. Rev. B **82**, 115314 (2010).
[19] C. M. Finch, V. M. Garcia-Suarez, and C. J. Lambert, Giant thermopower and figure of merit in single-molecule devices, Phys. Rev. B **79**, 033405 (2009).
[20] L. D. Hicks and M. S. Dresselhaus, Thermoelectric figure of merit of a one-dimensional quantum wire, Phys. Rev. B **47**, 16631 (1993).
[21] A. I. Boukai, Y. Bunimovich, J. Tahir-Kheli, J-K. Yu, W. A. Goddard III, and J. R. Heath, Silicon nanowires as efficient thermoelectric materials, Nature (London) **451**, 168 (2008).
[22] A. I. Hochbaum, R. Chen, R. D. Delgado, W. Liang, E. C. Garnett, M. Najarian, A. Majumdar, and P. Yang, Enhanced thermoelectric performance of rough silicon nanowires, Nature (London) **451**, 163 (2008).
[23] R. Bossisio, G. Fleury, and J-L. Pichard, Gate-modulated thermopower in disordered nanowires, New J. Phys. **16**, 035004 (2014).
[24] B. Sothman, R. Sanchez, and A. N. Jordan, Thermoelectric energy harvesting with quantum dots, Nanotechnology **26**, 032001 (2015), and references therein.
[25] T. Nakanishi and T. Kato, Thermopower of a quantum dot in a coherent regime, J. Phys. Soc. Jpn. **76**, 034715 (2007).
[26] M Wierzbicki and R. Swirkowicz, Influence of interference effects on thermoelectric properties of double quantum dots, Phys. Rev. B **84**, 075410 (2011).
[27] A. N. Jordan, B. Sothmann, R. Sánchez, and M. Buttiker, Powerful and efficient energy harvester with resonant tunneling quantum dots, Phys. Rev. B **87**, 075312 (2013).
[28] S. F. Svensson, E. A. Hoffmann, N. Nakpathomkun, P. M. Wu, H. Q. Xu, H. A. Nilsson, D. Sanchez, V. Kashcheyevs, and H. Linke, Nonlinear thermovoltage and thermocurrent in quantum dots, New J. Phys. **15**, 105011 (2013).
[29] S. Hershfield, K. A. Muttalib, and B. J. Nartowt, Nonlinear thermoelectric transport: A class of nanodevices for high efficiency and large power output, Phys. Rev. B **88**, 085426 (2013).
[30] R. S. Whitney, Most Efficient Quantum Thermoelectric at Finite Power Output, Phys. Rev. Lett. **112**, 130601 (2014).
[31] R. S. Whitney, Nonlinear thermoelectricity in point-contacts at pinch-off: A catastrophe aids cooling, Phys. Rev. B **88**, 064302 (2013).
[32] N. Nakpathomkun, H. Q. Xu, and H. Linke, Thermoelectric efficiency at maximum power in low-dimensional systems, Phys. Rev. B **82**, 235428 (2010).
[33] M. Zebarjadi, K. Esfarjani, and A. Shakouri, Nonlinear Peltier effect in semiconductors, Appl. Phys. Lett. **91**, 122104 (2007).
[34] B. Muralidharan and M. Grifoni, Performance analysis of an interacting quantum dot thermoelectric setup, Phys. Rev. B **85**, 155423 (2012).
[35] J. Meair and P. Jacquod, Scattering theory of linear thermoelectricity in quantum coherent conductors, J. Phys. Condens. Matter **25**, 082201 (2013).
[36] Y. M. Brovman, J. P. Small, Y. Hu, Y. Fang, C. M. Lieber, and P. Kim, Electric field effect thermoelectric transport in individual silicon and germanium/silicon nanowires, arXiv:1307.0249.
[37] M. Cutler and N. F. Mott, Observation of Anderson localization in an electron gas, Phys. Rev. **181**, 1336 (1969).
[38] R. Stadler and T. Markussen, Controlling the transmission lineshape of molecular t-stubs and potential thermoelectric applications, J. Chem. Phys. **135**, 154109 (2011).
[39] See, e.g., S. Datta, *Electronic Transport in Mesoscopic Systems* (Cambridge University Press, Cambridge, 1995).
[40] P. Lloyd, Exactly solvable model of electronic states in a three-dimensional disordered Hamiltonian: Non-existence of localized states, J. Phys. C **2**, 1717 (1969).
[41] See, e.g., L. E. Reichl, *The Transition to Chaos* (Springer-Verlag, New York, 1992).
[42] G. Y. Hu and R. F. O'Connell, Analytical inversion of symmetric tridiagonal matrices, J. Phys. A **29**, 1511 (1996).
[43] G. L. Pollack, Kapitza resistance, Rev. Mod. Phys. **41**, 48 (1969).
[44] E. T. Swartz and R. O. Pohl, Thermal boundary resistance, Rev. Mod. Phys. **61**, 605 (1989).
[45] M. P. Blencowe, Quantum energy flow in mesoscopic dielectric structures, Phys. Rev. B **59**, 4992 (1999).
[46] L. G. C. Rego and G. Kirczenow, Quantized Thermal Conductance of Dielectric Quantum Wires, Phys. Rev. Lett. **81**, 232 (1998).
[47] R. Bosisio, C. Gorini, G. Fleury, and J.-L. Pichard, Using Activated Transport in Parallel Nanowires for Energy Harvesting and Hot-Spot Cooling, preceding paper, Phys. Rev. Applied **3**, 054002 (2015).